

# First Results of the TOPSAR C-Band / L-Band Interferometer: Calibration and Differential Penetration

Paul A. Rosen and Scott F. Hensley

Jet Propulsion Laboratory  
California Institute of Technology  
4800 Oak Grove Drive  
Pasadena, CA 91109

JPL Airborne Earth Science Workshop  
March 4-8, 1996

## SUMMARY

The NASA /JPL TOPSAR instrument recently was extended from a single-wavelength C-band (5.6 cm- $\lambda$ ) dual aperture synthetic aperture radar interferometer to include a second wavelength at L-band (24 cm). Adding the second wavelength invites comparison of wavelength-diverse effects in topographic mapping of surfaces, with the principal goal of understanding the penetration of the radar signals in vegetation canopies, and determining the inferred topographic height. A first analysis of these data was conducted at two sites. Elkhorn Slough near Monterey, California presented flat, vegetation free terrain required for calibrating the radar interferometric parameters. A second site stretching from San Jose to Santa Cruz, CA, which is heavily vegetated, provided the first test case for wavelength diverse penetration studies. Preliminary results show that: a) the interferometer calibration determined at Elkhorn Slough is extendable to Laurel Quad and gives confidence in the C- and L-band height measurements; b) Clear differences are observed between the C- and L-band heights associated with vegetation, with C-band-derived topographic heights generally higher than those from L-band. The noise level in the L-band interferometer is presently the limiting factor in penetration studies.

## Introduction

The NASA/JPL TOPSAR instrument, maintained and operated by the Jet Propulsion Laboratory AIRSAR group (Yunjin Kim, supervisor) was extended from a C band-only topographic mapping SAR interferometer to L-band wavelengths (Howard Zebker, principal investigator) with the addition of a second L-band antenna complementing the All- $\{SAR\}$  polarimetry aperture. The radar instrumentation was modified to allow operation in the usual TOPSAR mode, in which a single antenna transmits the radar pulses and both antennas receive, or in ping-pong mode, where alternate antennas transmit on alternate pulses but both antennas receive on all pulses. In ping-pong mode, the effective separation between the antennas, called the baseline is increased by a factor of two relative to TOPSAR mode, giving increased sensitivity to topographic height. This is particularly important at L-band, where the short baseline relative to the wavelength causes considerable height noise despite good signal-to-noise conditions. Typical imaging geometries and height sensitivities for TOPSAR are summarized in Table 1.

The dual-wavelength, dual-baseline capability of the new TOPSAR system allows detailed study of the effects of vegetation canopies on the interferometrically derived heights. Coherent backscatter of microwave radiation is dominated by scatterers sized of the order of the radar wavelength.

It is well known from comparison of heights at field/forest stand boundaries in flat terrain that the C-band signal scattering in the forest is dominated by the canopy such that the interferometrically derived height is well above the forest base. The dual wavelength capability of the interferometer measures the differential penetration depth (if any) to provide insight into the scattering mechanism, which can be complicated in real canopies. The vegetation canopy increases the effective scattering area of each resolution cell, leading to increasingly decorrelated radar echoes as the interferometer baseline is increased. The dual baseline capability of the TOPSAR interferometer tests this prediction and establishes the usefulness of decorrelation measurements for estimating canopy depths.

This work takes the first steps toward addressing these fundamental questions by first calibrating the system at C- and L-band, then comparing C- and L-band height maps. Before the measurements can be interpreted, calibration is essential. The locations of the phase centers of the interferometer antennas are very difficult to measure at the millimeter scale required for accurate topographic mapping (Madsen et al 1993). Centimeter scale errors in baseline components can lead to planimetric and vertical map distortions in the tens of meters. In addition to the baseline, systematic phase errors exist in the radar data that are attributable to scattering of energy into an antenna from multiple paths, ostensibly the antenna farings. These systematic phase errors corrupt the derived height maps in the cross track direction with vertical and horizontal oscillations of several meters' amplitude at C-band and over 10 meters at L-band, severely limiting the utility of the measurements for sensitive differential penetration studies.

## Calibration

The C-band TOPSAR baseline is measured yearly to an accuracy of a few centimeters. Until recently inaccuracies in the aircraft attitude and position measurement system precluded meter scale accuracy mapping. With the operational use of a refined inertial navigation system in late 1994 and in 1995, a finer accuracy baseline for C-band is needed. Calibration using an array of corner reflectors in Rosamond dry lake bed is under way, however the flight conditions were turbulent and windy, so verifying the derived baseline parameters will require additional work. For the purposes of this study an alternate path of calibration was taken. It has the advantage of removing height distortions due to baseline errors and multipath phase errors simultaneously. This phase screen approach was first employed when JPL calibrated the Environmental Research Institute of Michigan's ISAR X-band topographic mapper (Kim and Inel 1995).

The phase screen approach requires a reference digital elevation model. The TOPSAR digital terrain map is computed as an array of height values on a locally spherical grid. At the same time, the imaging geometry of each array element is recorded. The difference between the TOPSAR map and the reference DEM is taken - this constitutes an array of height errors. The residual interferometric phase error needed for calibration  $\Delta\Phi$  is related to these height errors  $\Delta h$  through the ambiguity height equation, given in a simplified two dimensional geometry by

$$\Delta\Phi(r) = \frac{2\pi n B \cos(\theta - \alpha)}{\lambda r \sin(\theta)} \Delta h \quad (0.1)$$

where  $B$  is the baseline length,  $\alpha$  is the angle the baseline makes with the horizontal measured counterclockwise,  $\theta$  is the look angle,  $\lambda$  is the wavelength, and  $n$  is 1 for TOPSAR mode or 2 for ping-pong mode. The height-induced errors from both multipath and baseline error are primarily

functions of the look angle, so the phase screen correction inferred from the difference 1 DEM and the geometry is tabulated as a function of lookangle. By using the entire two dimensional 1 DEM, the one dimensional phase screen benefits from averaging and is quite smooth despite errors in the 1 DEM data. Using this phase screen to correct the interferogram, a new TOPSAR digital terrain map is produced and compared to the reference DEM. An adjusted phase screen is then computed and compared to the first estimate. This procedure is iterated until the phase screen becomes stable, **usually** after no more than two iterations

Figure 1 illustrate the phase distortions in the radar heights in the left-most panel. The area is located at Elkhorn Slough, CA and is quite flat, containing a large part of Monterey Bay in the left of the image. Despite the flat terrain, there is a tilt of the heights from left to right (near range to far range) in the image as well as oscillatory banding aligned with the flight direction, the effects of baseline error and multipath. The center panel shows the difference between the radar heights and the USGS 90m DEM resampled to the radar coordinates at 30 m spacing. The USGS 1 DEM is the best readily available digital data set for this site. Nearly all the terrain features remaining in the difference map are due to inaccuracies or resolution limits in the USGS data. Nevertheless, the net phase screen derived from the difference map is quite smooth.

On the second iteration, the region of the difference map used was restricted to the ocean anti featureless areas in the bottom half of the image. This improved the estimate considerably. The right most panel of Fig. 1 **shows** the calibrated height data. The ripples in the Bay and flat regions clearly evident in the left panel have been removed in the right panel. If we assume that the average height of the USGS map over wide areas is correct, we can conclude that the phase screen calibration performed well. Figure 2 shows the phase screen profile as a function of look angle.

The L-band system is new, so the baseline is commensurately less well known than the C-band baseline. To calibrate L-band, we decided to estimate its baseline by comparing the interferometric phase at C-band to the phase at L-band. If both baselines are perfectly well known then the following relationship holds:

$$\Phi_L(r) - \frac{\lambda_C B r \cos(\theta(r))}{\lambda_L B_C \cos(\theta(r))} \frac{\alpha_C}{\alpha_L} \Phi_C(r) = 0 \quad (0.2)$$

Any residual phase  $d\Phi(r)$  remaining as a function of range  $r$  we attribute at this stage to baseline error through the relation

$$\frac{\lambda}{2\pi n} d\Phi(r) = dB \sin(\theta - \alpha) - d\alpha B \cos(\theta - \alpha) \quad (0.3)$$

It is straightforward to derive the corrections  $dB$  and  $d\alpha$  from the residuals  $d\Phi$ . The L-band baseline given in Table 2 was determined in this way. As a cross check of the baseline estimate, we measured planimetric distortion of the data before and after baseline correction by correlating the L-band interferogram with the C-band data. Before baseline correction, the images were misregistered by many pixels particularly in the near range. After baseline correction, the images aligned to within a pixel everywhere.

The phase screen correction for L-band is still necessary because of multipath. Instead of using the USGS DEM, we used the newly calibrated C-band DEM. Few large scale artifacts exist in the difference map, however the large amount of height noise in the L-band data due to large ambiguity height limited the effectiveness of the phase screen. Residual multipath ripples remain in the L-band 1 DEM at the 1-2 meter amplitude level. Though this is considerably lower than the statistical height noise at L-band, the artifacts are visible to the eye.

## Preliminary penetration results

Two differential penetration maps have been produced. The first is located at Elkhorn Slough, an obvious choice for calibration because the surface is essentially unvegetated. Figure 3 shows the calibrated C-band (left panel), L- band (center) and the C-L height difference (right panel). We expect the right panel to have no topographic variation even in areas of high relief, and this is observed: The L-band calibration succeeded, and the statistical height error of 2 - 5 m is sufficiently low to allow detection of penetration differences.

Figure 4 shows the same three panels for a different site, Laurel Quad, CA located between San Jose and Santa Cruz. Laurel Quad is heavily vegetated with tall conifers and deciduous trees, as well as populated with grasslands and clear-cuts. Penetration differences should be apparent in the C-L difference map as positive numbers because penetration is expected to be larger at L- band. Indeed, close examination of the right panel shows virtually no height differences in the urban areas to the north and south but statistically significant differences in the forested areas between. Note that the imaging geometry and acquisition time for the C- and L-band systems are identical so there can be no terrain bias effect or angular calibration error causing this difference. Furthermore, careful study of the figure, or inspection of the full resolution data (these data are averaged for display), shows a clear correlation between backscatter variations associated with canopy and the height differences. In particular, above the image center southeast of San Jose, the northern slopes show clear vegetation, while the southern slopes are bare and show no vegetation.

Transects through the urban areas and forest consisting of profiles averaged across many image lines show clear distinctions, with an average difference of zero in the city and 4-6 meters in the forest. It is not clear how representative the average transect height is of the actual penetration locally. The image shows patchiness that is often attributable to variations in canopy. Because of the large height error in the L band data however, considerable averaging is required. Therefore, to better characterize the penetration, uniform tree stands must be identified from ortho images and other ground truth and a statistical average computed, probably as a single number per stand. This detailed analysis is underway. Comparison of these data with other acquisition modes will also provide insights into penetration phenomenology. However, calibration of the remaining modes is just beginning.

## References

1. Kim, Y. and D. Imel (1995) IFSAR/E Phase Calibration Report. JPL Interoffice Memorandum 3349-95-017 (internal document) Jet Propulsion Laboratory, Pasadena, Calif.
2. Madsen S.N., H. A. Zebker, and J. M. Martin (1993). Topographic mapping using radar interferometry: processing techniques. *IEEE Trans. Geosci. Rem. Sens.*, **31**, 246-256.

## Acknowledgment

The research described in this paper was carried out by the Jet Propulsion Laboratory, California Institute of Technology, under a contract with the National Aeronautics and Space Administration.

TABLE 1  
RELEVANT INTERFEROMETRIC MAPPING MODES AND PARAMETERS<sup>†</sup>

Map Product posting (m)		5
Map Product Resolution (m)		15
Range Bandwidth (MHz)		40
Range Resolution (m)		3.331
1 Pulse Repetition Ground Spacing (m)		0.34
Number of Looks		30
Aircraft Altitude (km)		8
Range (km)	9	17.5
Look Angle (deg)	25	63
C/L-band Ambiguity Height (m)	56/243	1.74/755
C/L-band Nominal Interferometric Correlation	0.90/0.94	0.90/0.94
C/L-band Nominal Statistical Height Error (m)	0.56/1.81	1.73/5.63

<sup>†</sup> For 40 MHz ping-pong mode

TABLE 2  
PRELIMINARY TOPSAR INTERFEROMETRIC CALIBRATION PARAMETERS

Wave length	L-Band (24 cm)			C-band (5.6 cm)		
Antenna Location	1b)	Bottom	T-B <sup>a</sup>	Top	Bottom	T-B
X <sup>†</sup> (m)	0.54	0.54	0	2.46	2.46	0
Y (m)	1.231	0.52	0.711	1.154	0.157	0.997
Z (m)	1.601	- 0.23	1.831	1.577	- 0.717	2.294
$\Delta\phi_d$ (rad) <sup>††</sup>	0.85	0	0.85	0	- 1.35	1.35
$\Delta t_d$ (ns)	428.02	444.72	16.7	406.08	437.04	- 30.96

<sup>a</sup> T-B implies baseline components

<sup>†</sup> X coordinate measured forward along aircraft fuselage

Y coordinate measured outward to port side

Z coordinate measured vertically upward

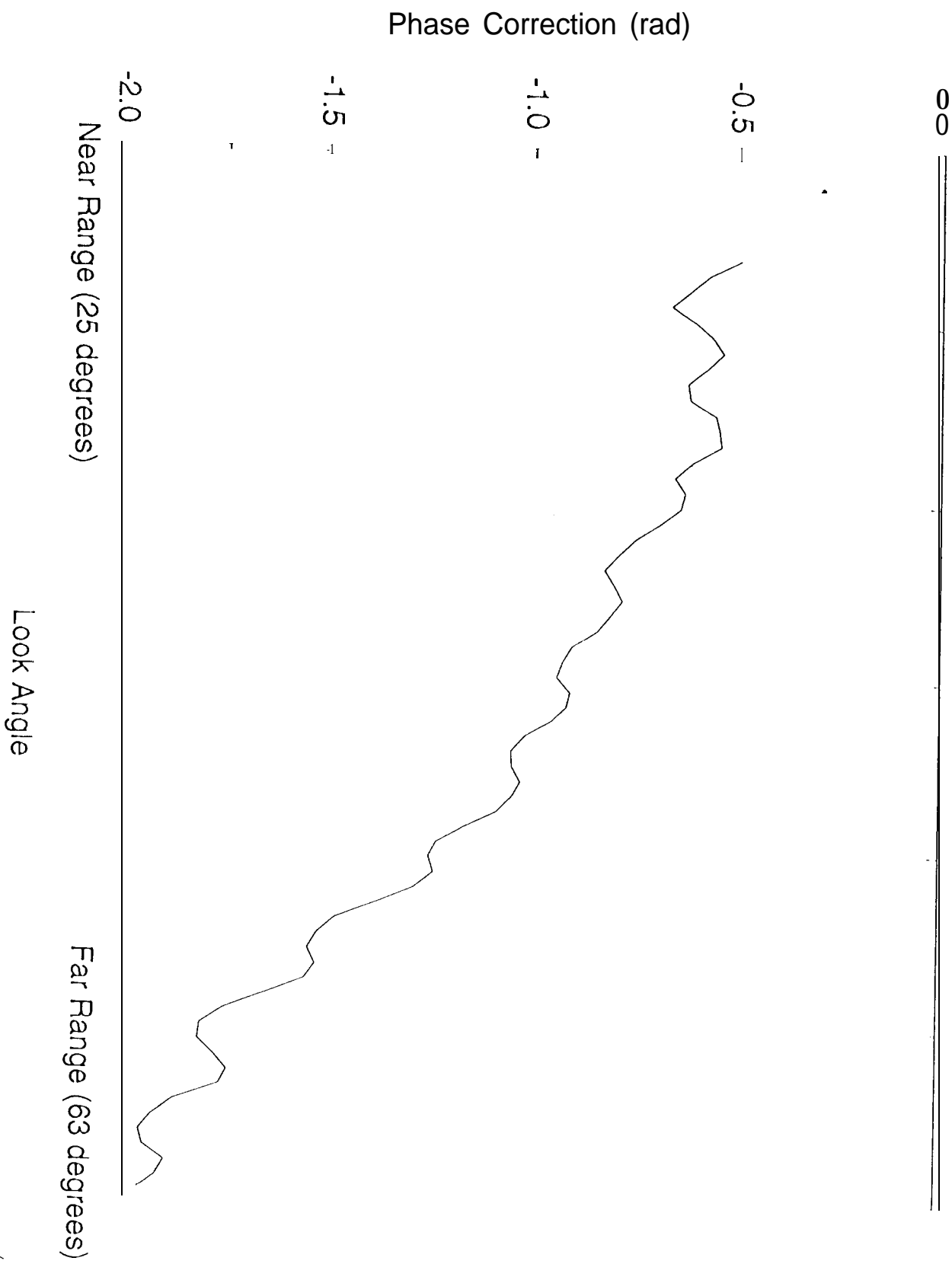
<sup>††</sup> Channel phase  $\Delta\phi_d$  and time delay  $\Delta t_c$  are mode dependent.

These values are valid for 40 MHz ping pong mode only.

# Phase Screen Calibration

C-Band Phase Correction Vector

FIGURE 2

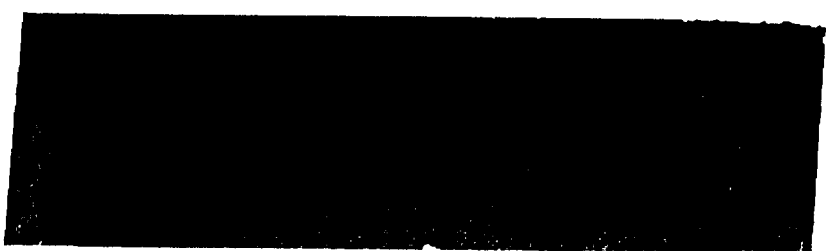


TOPSAR "PHASE SCREEN" CALIBRATION  
Elkhorn Slough, CA Run 180-1 1995

C-BAND (5.6 cm  $\lambda$ )  
TOPSAR DTE

TOPSAR DTE  
USGS 90 M DTM  
DIFFERENCE

TOPSAR DTE  
AFTER CALIBRATION



Height  
Scale  
20 m

JPL Figure 1

TOPSAR DUAL FREQUENCY TOPOGRAPHIC MAPPING  
Elkhorn Slough, CA Run180-1 1995

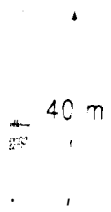
C-BAND (5.6 cm  $\lambda$ )

L-B AND (24 cm  $\lambda$ )

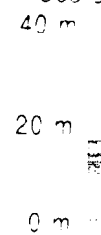
C-L TOPOGRAPHY



Height  
Scale



Height  
Difference  
Scale



JPL Figure 3



# TOPSAR DUAL FREQUENCY TOMOGRAPHIC MAPPING

LaurelQuad. CA < Ru180-31995

C-BAND (5.6 cm  $\lambda$ )

L-BAND(24 cm  $\lambda$ )

C-L TOPOGRAPHY



San Jose

Height  
Scale

100 m

Santa Cruz



Height  
Difference  
Scale

40 m

20 m

0 m

